Report

Current Biology

Neural control of fluid homeostasis is engaged below 10°C in hibernation

Graphical abstract

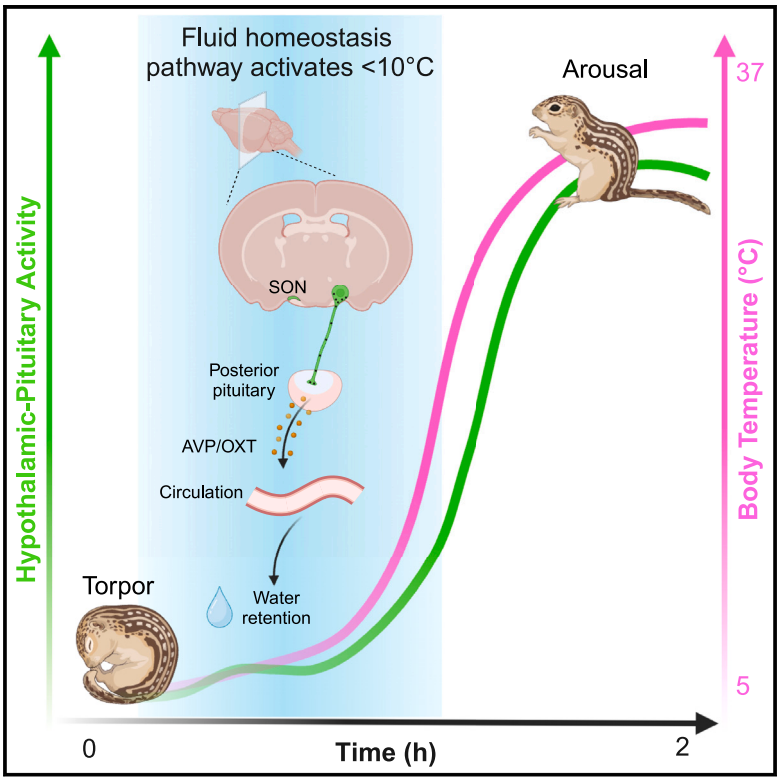

Authors

Madeleine S. Junkins, Ni Y. Feng, Lyle A. Murphy, Genevieve Curtis, Dana K. Merriman, Sviatoslav N. Bagriantsev, Elena O. Gracheva

Correspondence

nfeng@wesleyan.edu (N.Y.F.), slav.bagriantsev@yale.edu (S.N.B.), elena.gracheva@yale.edu (E.O.G.)

In brief

Junkins, Feng et al. use fiber photometry to show that neural activity can occur below 10°C in hibernating squirrels. The activity of supraoptic nucleus neurons at such low temperatures permits the release of vasopressin and oxytocin into the bloodstream, thus promoting water retention during the dramatic transition from torpor to arousal.

Highlights

- Fiber photometry in an obligatory hibernator during the torpor-arousal transition
- *In vivo* evidence of osmosensory neural activity below 10°C
- Hypothalamic-pituitary axis is engaged at 10°C
- Mechanism for water conservation during hibernation

Junkins et al., 2024, Current Biology *34*, 1–8
February 26, 2024 © 2024 Elsevier Inc.
https://doi.org/10.1016/j.cub.2024.01.035

CellPress

Please cite this article in press as: Junkins et al., Neural control of fluid homeostasis is engaged below 10°C in hibernation, Current Biology (2024), https://doi.org/10.1016/j.cub.2024.01.035

Current Biology

CellPress

Report

Neural control of fluid homeostasis is engaged below 10°C in hibernation

Madeleine S. Junkins,[1,2,3,9] Ni Y. Feng,[1,2,3,7,8,9,*] Lyle A. Murphy,[1] Genevieve Curtis,[5] Dana K. Merriman,[6] Sviatoslav N. Bagriantsev,[1,10,*] and Elena O. Gracheva[1,2,3,4,11,*]

[1]Department of Cellular and Molecular Physiology, Yale University School of Medicine, 333 Cedar Street, New Haven, CT 06510, USA
[2]Department of Neuroscience, Yale University School of Medicine, 333 Cedar Street, New Haven, CT 06510, USA
[3]Department of Neuroscience and Program in Cellular Neuroscience, Neurodegeneration and Repair, Yale University School of Medicine, 333 Cedar Street, New Haven, CT 06510, USA
[4]Kavli Institute for Neuroscience, Yale University School of Medicine, 333 Cedar Street, New Haven, CT 06510, USA
[5]Department of Biology, Wesleyan University, 52 Lawn Ave, Middletown, CT 06459, USA
[6]Department of Biology, University of Wisconsin-Oshkosh, 800 Algoma Blvd, Oshkosh, WI 54901, USA
[7]Neuroscience & Behavior Program, Wesleyan University, 52 Lawn Ave, Middletown, CT 06459, USA
[8]Present address: Department of Biology, Wesleyan University, 52 Lawn Ave, Middletown, CT 06459, USA
[9]These authors contributed equally
[10]X (formerly Twitter): @SlavBagria
[11]Lead contact
*Correspondence: nfeng@wesleyan.edu (N.Y.F.), slav.bagriantsev@yale.edu (S.N.B.), elena.gracheva@yale.edu (E.O.G.)
https://doi.org/10.1016/j.cub.2024.01.035

SUMMARY

Thirteen-lined ground squirrels (*Ictidomys tridecemlineatus*) hibernate for several months each winter without access to water,[1] but the mechanisms that maintain fluid homeostasis during hibernation are poorly understood. In torpor, when body temperature (T_B) reaches 4°C, squirrels decrease metabolism, slow heart rate, and reduce plasma levels of the antidiuretic hormones arginine vasopressin (AVP) and oxytocin (OXT).[1] Squirrels spontaneously undergo interbout arousal (IBA) every 2 weeks, temporarily recovering an active-like metabolism and a T_B of 37°C for up to 48 h.[1,2] Despite the low levels of AVP and OXT during torpor, profound increases in blood pressure and heart rate during the torpor-IBA transition are not associated with massive fluid loss, suggesting the existence of a mechanism that protects against diuresis at a low T_B. Here, we demonstrate that the antidiuretic hormone release pathway is activated by hypothalamic supraoptic nucleus (SON) neurons early in the torpor-arousal transition. SON neuron activity, dense-core vesicle release from the posterior pituitary, and plasma hormone levels all begin to increase before T_B reaches 10°C. *In vivo* fiber photometry of SON neurons from hibernating squirrels, together with RNA sequencing and c-FOS immunohistochemistry, confirms that SON is electrically, transcriptionally, and translationally active to monitor blood osmolality throughout the dynamic torpor-arousal transition. Our work emphasizes the importance of the antidiuretic pathway during the torpor-arousal transition and reveals that the neurophysiological mechanism that coordinates the hormonal response to retain fluid is active at an extremely low T_B, which is prohibitive for these processes in non-hibernators.

RESULTS AND DISCUSSION

In all forms of life, challenges such as resource deprivation have necessitated the evolution of coping mechanisms. One notable strategy is hibernation, which allows some animals to survive without food, water, or warmth for an entire winter.[2–5] For small mammals, hibernation is characterized by the alternation between two physiological states: torpor and interbout arousal (IBA). During torpor, metabolic and respiratory rates are profoundly suppressed and body temperature (T_B) drops to ambient levels—as low as 2°C–4°C.[1,2,6] Torpor bouts last up to 2 weeks, but are regularly interrupted by spontaneous IBAs during which physiological parameters return to active-like levels for up to 48 h.[2–5] Though many features of hibernation have been characterized, a complete mechanistic understanding of the molecular and neurophysiological processes that enable this phenomenon remains elusive.[7]

In non-hibernating mammals, water deprivation leads to elevated serum osmolality, increased circulating levels of the antidiuretic hormones arginine vasopressin (AVP) and oxytocin (OXT), and the induction of thirst.[8–11] AVP and OXT enhance water reabsorption and urine concentration in the kidneys.[8] Recently, we discovered that, despite months-long water deprivation, torpid thirteen-lined ground squirrels (13LGS) do not experience these canonical signs of dehydration. Instead, they lower their serum osmolality and decrease plasma AVP and OXT concentrations to undetectable levels.[1] In IBA, squirrels recover an active-like serum osmolality and antidiuretic hormone concentration, but they do not surpass these levels as would be expected in the context of long-term water deprivation.[1] Furthermore, IBA squirrels exhibit a near-complete avoidance of water drinking.[1] This unconventional relationship between blood biochemistry, hormone release, and behavior may enable water

Please cite this article in press as: Junkins et al., Neural control of fluid homeostasis is engaged below 10°C in hibernation, Current Biology (2024), https://doi.org/10.1016/j.cub.2024.01.035

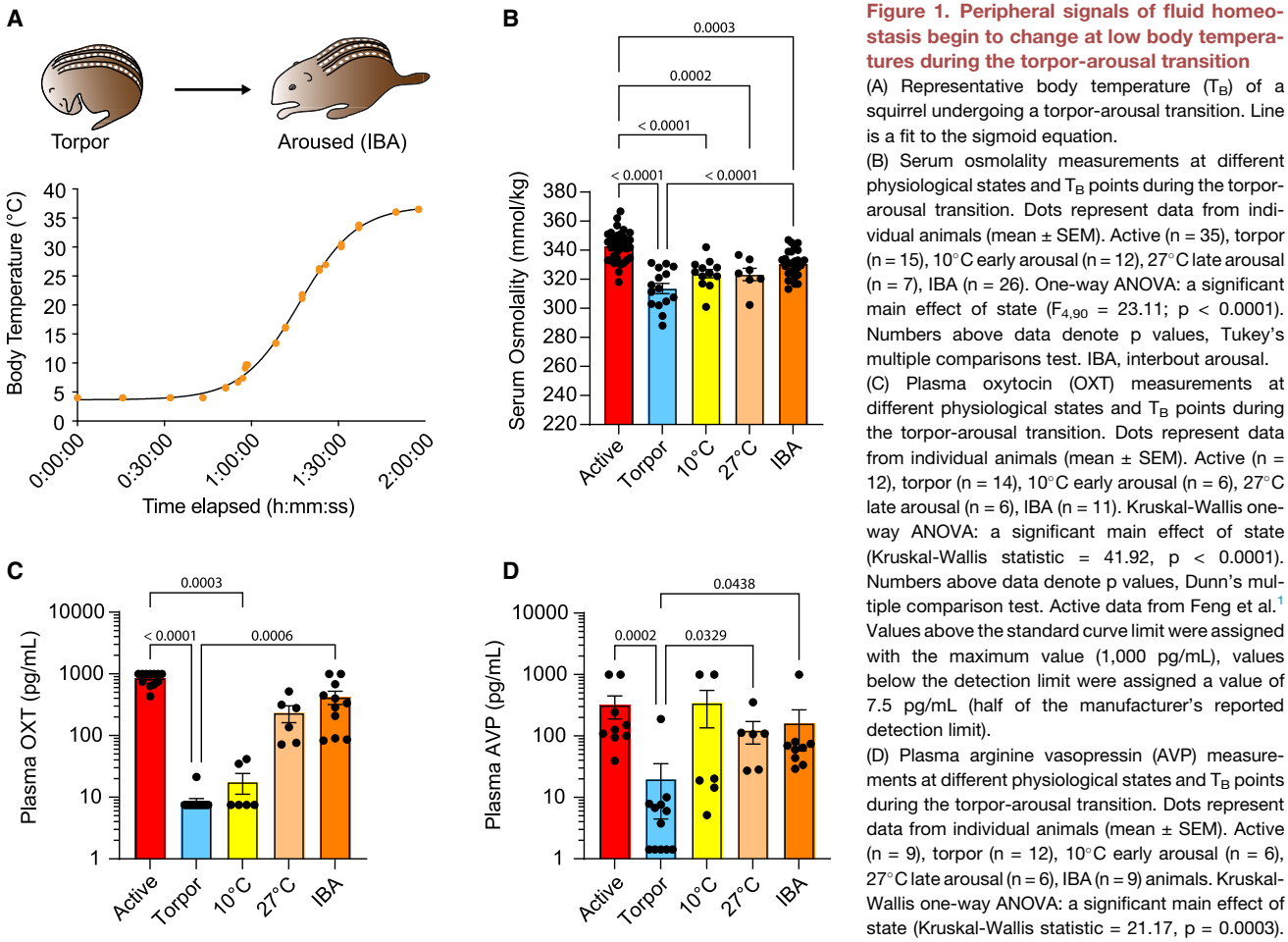

Figure 1. Peripheral signals of fluid homeostasis begin to change at low body temperatures during the torpor-arousal transition

(A) Representative body temperature (T_B) of a squirrel undergoing a torpor-arousal transition. Line is a fit to the sigmoid equation.

(B) Serum osmolality measurements at different physiological states and T_B points during the torpor-arousal transition. Dots represent data from individual animals (mean ± SEM). Active (n = 35), torpor (n = 15), 10°C early arousal (n = 12), 27°C late arousal (n = 7), IBA (n = 26). One-way ANOVA: a significant main effect of state ($F_{4,90}$ = 23.11; p < 0.0001). Numbers above data denote p values, Tukey's multiple comparisons test. IBA, interbout arousal.

(C) Plasma oxytocin (OXT) measurements at different physiological states and T_B points during the torpor-arousal transition. Dots represent data from individual animals (mean ± SEM). Active (n = 12), torpor (n = 14), 10°C early arousal (n = 6), 27°C late arousal (n = 6), IBA (n = 11). Kruskal-Wallis one-way ANOVA: a significant main effect of state (Kruskal-Wallis statistic = 41.92, p < 0.0001). Numbers above data denote p values, Dunn's multiple comparison test. Active data from Feng et al.[1] Values above the standard curve limit were assigned with the maximum value (1,000 pg/mL), values below the detection limit were assigned a value of 7.5 pg/mL (half of the manufacturer's reported detection limit).

(D) Plasma arginine vasopressin (AVP) measurements at different physiological states and T_B points during the torpor-arousal transition. Dots represent data from individual animals (mean ± SEM). Active (n = 9), torpor (n = 12), 10°C early arousal (n = 6), 27°C late arousal (n = 6), IBA (n = 9) animals. Kruskal-Wallis one-way ANOVA: a significant main effect of state (Kruskal-Wallis statistic = 21.17, p = 0.0003). Numbers above data denote p values, Dunn's multiple comparison test. Active data from Feng et al.[1] Values above the standard curve limit were assigned with the maximum value (1,000 pg/mL), values below the detection limit were assigned a value of 1.42 pg/mL (half of the manufacturer's reported detection limit).

retention by the kidneys while suppressing the drive to leave the safety of the underground burrow in search of water.

The torpor-IBA transition is a critical time during which physiological parameters change over 1–2 h, including dramatic rises in serum osmolality and mean arterial pressure.[1,12,13] Thus, hibernators must balance between preventing water loss caused by pressure diuresis and the need to excrete waste through urine production during each arousal. Because 13LGS experience 20–30 torpor-arousal transitions and do not drink water during hibernation, they cannot afford unnecessary fluid excretion.[1,6] Indeed, by the time IBA is reached, circulating antidiuretic hormones return to active-like levels from the minimum concentrations observed during torpor.[1] However, how early fluid homeostatic mechanisms are engaged during the torpor-arousal transition is unknown. Here, we explored the hypothesis that the neuronal control of antidiuretic hormone release commences at extremely low T_B during the transition from torpor to IBA.

Peripheral signals of fluid homeostasis change dynamically at 10°C

Classic peripheral readouts of fluid homeostasis include serum osmolality and plasma levels of AVP and OXT.[8,10] Peripheral AVP and OXT play complementary roles in the context of fluid homeostasis by promoting renal water retention and urine concentration in response to increases in serum osmolality.[14,15] To assess peripheral and central readouts of hormone release across the torpor-arousal transition (Figure 1A), we collected and analyzed blood and neural tissues during early (T_B = 10°C) and late (T_B = 27°C) stages of this process. We observed that mean serum osmolality increased by ~10 mOsm from torpor to 10°C and again by ~10 mOsm from 27°C to 37°C in IBA (Figure 1B). Such an early increase in serum osmolality likely reflects the release of metabolites into circulation as physiological processes begin to speed up.[1] Because squirrels in early arousal also experience a profound elevation in blood pressure, we hypothesized that the antidiuretic hormones would begin to rise even at 10°C to prevent water loss through diuresis.[12,13] Indeed, we found that mean plasma levels of OXT nearly doubled from 8.49 ± 0.99 pg/mL (mean ± SE) in torpor to 17.72 ± 6.53 pg/mL at 10°C and reached a near-IBA level by 27°C (233.0 ± 70.99 pg/mL at 27°C, 419.5 ± 102.1 in IBA; torpor vs. IBA, p = 0.0006, Dunn's multiple comparisons test; Figure 1C). Similarly, mean AVP levels increased from 19.85 ± 15.41 pg/mL in torpor to 343.1 ± 207.7 pg/mL at 10°C, to 122.8 ± 48.88 pg/mL at 27°C

Please cite this article in press as: Junkins et al., Neural control of fluid homeostasis is engaged below 10°C in hibernation, Current Biology (2024), https://doi.org/10.1016/j.cub.2024.01.035

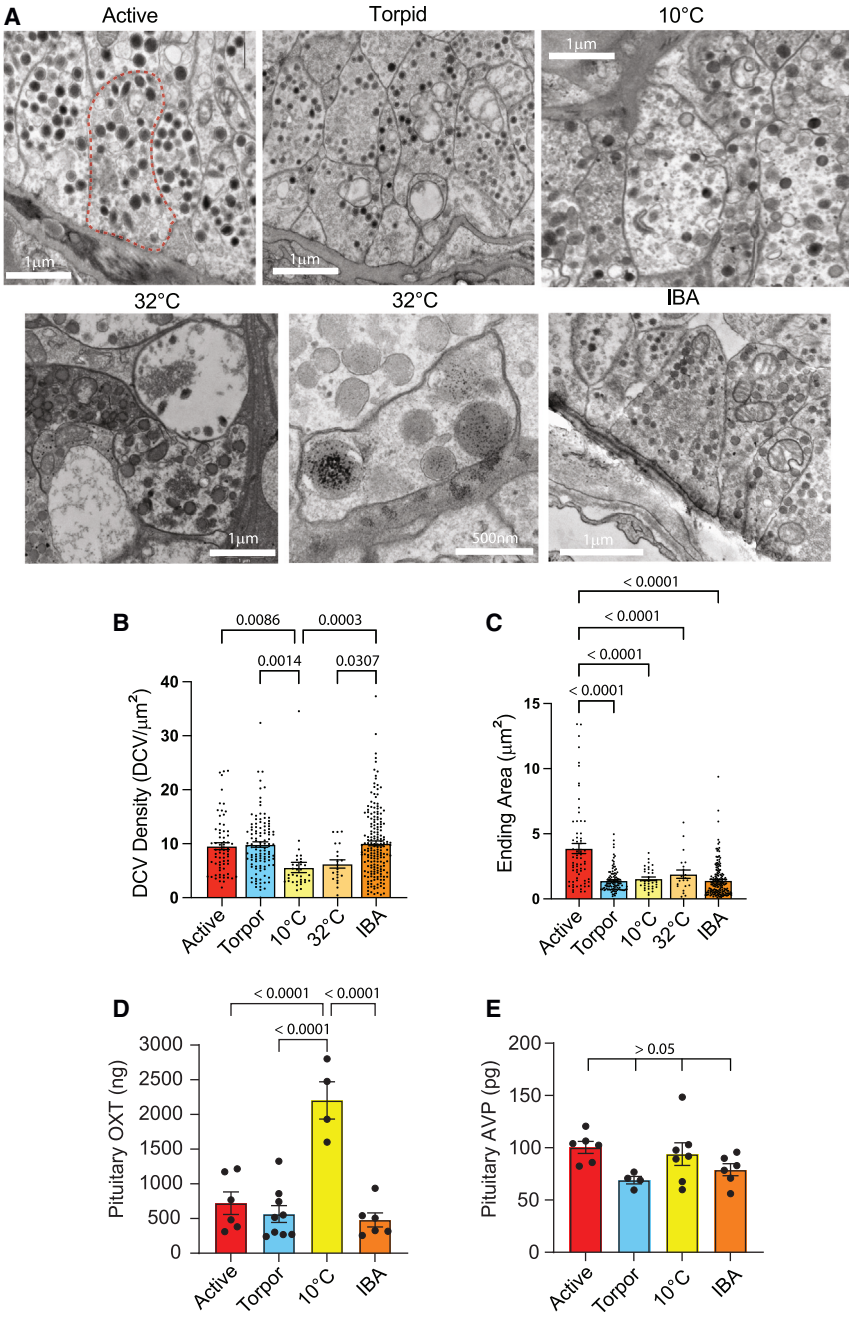

Figure 2. Posterior pituitary EM supports active release of stored peptide vesicles during arousal

(A) Exemplar electron micrographs of large dense-core vesicles (DCVs) in neurosecretory axonal endings of posterior pituitary from squirrels at different physiological states. Dotted red line in active panel denotes a single neurosecretory ending.

(B) Quantification of dense-core vesicle density measured from squirrels taken at different physiological states: active (n = 3), torpor (n = 3), 10°C early arousal (n = 2), 32°C late arousal (n = 2), IBA (n = 4). Dots represent density measurements from individual axonal endings (mean ± SEM). One-way ANOVA: a significant main effect of state ($F_{4,418}$ = 6.237); p < 0.0001). Numbers above data denote p values, Tukey's multiple comparisons test.

(C) Quantification of the neurosecretory axonal endings area measured at different physiological states during the torpor-arousal transition. Active (n = 3), torpor (n = 3), 10°C early arousal (n = 2), 32°C late arousal (n = 2), IBA (n = 4). Dots represent measurements from individual axonal endings (mean ± SEM). One-way ANOVA: a significant main effect of state ($F_{4,418}$ = 31.43, p < 0.0001). Numbers above data denote p values, Tukey's multiple comparisons test.

(D) Quantification of pituitary oxytocin measured at different physiological states during the torpor-arousal transition. Dots represent data from individual animals (mean ± SEM). Active (n = 6), torpor (n = 9), 10°C early arousal (n = 4), IBA (n = 6). One-way ANOVA: a significant main effect of state ($F_{3,21}$ = 20.78, p < 0.0001). Numbers above data denote p values, Tukey's multiple comparisons test. Active and IBA data from Feng et al.[1]

(E) Quantification of pituitary vasopressin measured at different physiological states during the torpor-arousal transition. Dots represent data from individual animals (mean ± SEM). Active (n = 6), torpor (n = 4), 10°C early arousal (n = 7), IBA (n = 6). One-way ANOVA: no significant main effect of state ($F_{3,19}$ = 2.740, p = 0.0718). Numbers above data denote p values, Tukey's multiple comparisons test.

and 161.7 ± 105.0 pg/mL in IBA (torpor vs. 27°C, p = 0.0329; torpor vs. IBA, p = 0.0438, Dunn's multiple comparisons test; Figure 1D). These results reveal that a coordinated release of antidiuretic hormones during the torpor-arousal transition is underway by the time T_B of arousing squirrels reaches 10°C.

Peptide release from the posterior pituitary at 10°C

AVP and OXT are produced in magnocellular hypothalamic neurons in the supraoptic nucleus (SON) and paraventricular nucleus of the hypothalamus (PVH), whose neurosecretory terminals reside in the posterior pituitary.[8,16] Within these terminals, AVP and OXT are stored in dense-core vesicles (DCVs) and released into local and subsequently general circulation when serum osmolality increases.

To ascertain whether changes in plasma AVP and OXT during the torpor-arousal transition are mediated by this mechanism, we collected posterior pituitary samples at different T_B points across the hibernation cycle, including at the early (10°C) and late (32°C) stages during the torpor-arousal transition, and subjected them to ultrastructural analysis by transmission electron microscopy (EM) (Figure 2A). We found that while DCV density did not change between active and torpor states (9.55 ± 0.64 DCVs/µm² in active, 9.85 ± 0.49 DCVs/µm² in torpor; mean ± SE; p = 0.9971, Tukey's multiple comparisons test; Figure 2B), it significantly decreased between torpor and 10°C (5.59 ± 0.95 DCVs/µm² at 10°C; p = 0.0014). DCV density remained unchanged as squirrels warmed to 32°C but rebounded to active levels during IBA (10.06 ± 0.46 DCVs/µm² in IBA; p = 0.0003). Although axon

Please cite this article in press as: Junkins et al., Neural control of fluid homeostasis is engaged below 10°C in hibernation, Current Biology (2024), https://doi.org/10.1016/j.cub.2024.01.035

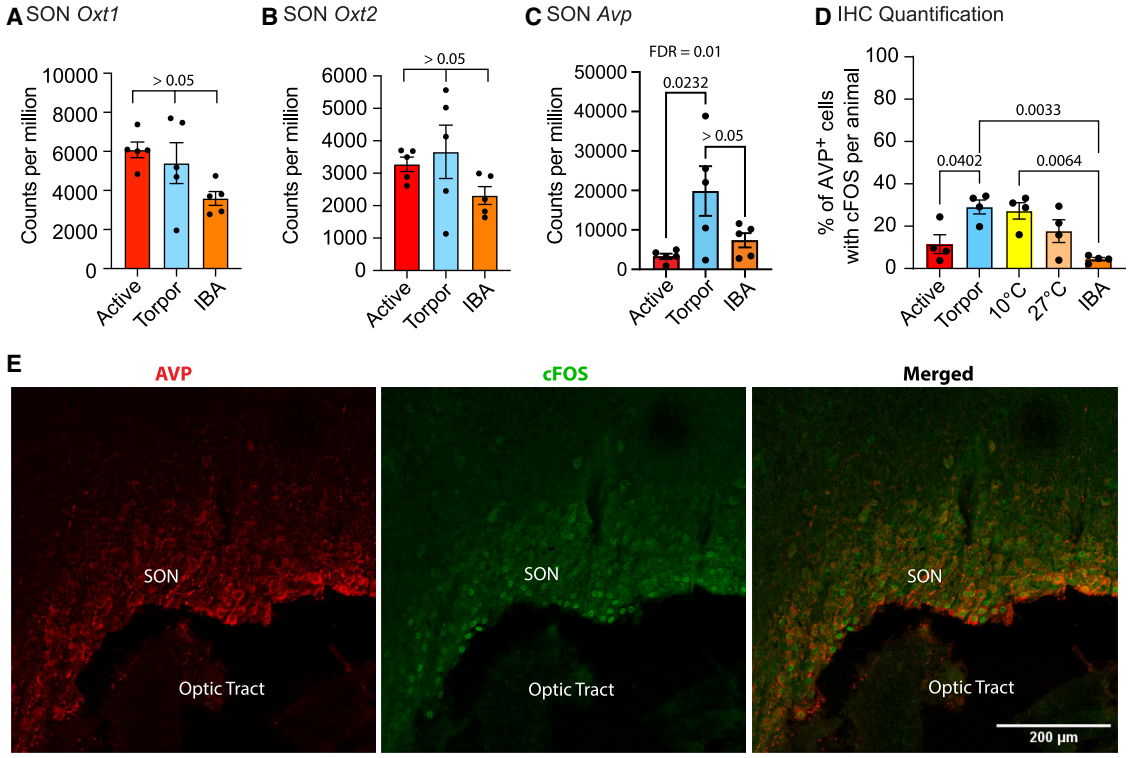

Figure 3. Biosynthetic activity in SON at 10°C

(A–C) Quantification of oxytocin (*Oxt1* and *Oxt2*) and arginine vasopressin (*Avp*) transcripts in SON of active, torpid, and IBA squirrels. Dots represent data from individual animals (mean ± SEM). Active (n = 5), torpor (n = 5), IBA (n = 5). One-way ANOVA: a significant main effect of state for *Avp* only ($F_{2,12} = 5.143$; p = 0.0244). Numbers above data denote p values, Tukey's multiple comparisons test.

(D) Quantification of immunohistochemistry (IHC) analysis of cells co-expressing AVP and c-FOS in SON at different stages during the torpor-arousal transition. Each dot represents the percentage of c-FOS$^+$ neurons among AVP$^+$ cells, quantified across 3–4 sections for individual animals (mean ± SEM). Active (n = 4), torpor (n = 4), 10°C early arousal (n = 4), 27°C late arousal (n = 4), IBA (n = 4). One-way ANOVA: a significant main effect of state ($F_{4,15} = 7.222$; p = 0.0019). Numbers above data denote p values, Tukey's multiple comparisons test.

(E) Exemplar immunohistochemical images showing AVP$^+$ (red) and c-FOS$^+$ (green) cells in SON of a squirrel with a T_B of 10°C during the torpor-arousal transition.

terminal area was smaller in torpid squirrels compared with active squirrels (3.87 ± 0.39 µm^2 in active; 1.399 ± 0.0835 µm^2 in torpor; p < 0.0001, Tukey's multiple comparisons test; Figure 2C), this did not change at any point during the torpor-arousal transition, confirming that DCV density changes were not due to terminal area changes, which likely reflect a seasonal difference. The observed changes in DCV density suggests that the posterior pituitary DCV pool is released during early arousal at 10°C, replenished during steady-state IBA, and stored during the ensuing torpor bout to be released in the next arousal cycle.

Next, we measured the total OXT and AVP content in the posterior pituitary, which contained sites of DCV storage in addition to the neurosecretory terminals.[16] We found that pituitary OXT concentration significantly increased from 526.3 ± 112.5 ng in torpor to 2,052 ± 250.7 ng at 10°C (p < 0.0001, Tukey's multiple comparisons test; Figure 2D). Pituitary AVP concentration increased by 36% from 69.04 ± 3.57 pg in torpor to 93.96 ± 10.85 pg at 10°C, though the effect was not statistically significant (p = 0.2028, Tukey's multiple comparisons test; Figure 2E). The increase in pituitary OXT and AVP content agrees with the observed changes in DCV density and likely reflects both the release of the hormones out of DCVs into local circulation as well as mobilization of DCVs from the neuronal soma in the hypothalamus to the sites of DCV storage in the posterior pituitary.[16] Notably, these events take place early during arousal when T_B has just reached 10°C.

Biosynthetic activity in SON at 10°C

Next, we asked whether oxytocinergic and vasopressinergic magnocellular neurons in SON accumulate *Oxt1/2* and *Avp* transcripts during IBA and/or store them during torpor. To test this, we performed bulk RNA sequencing of the SON across the hibernation cycle. The number of *Oxt1* and *Oxt2* transcripts did not significantly differ between states, remaining high in active, torpor, and IBA (Figures 3A and 3B). Interestingly, we detected a significant increase in the abundance of *Avp* transcripts in torpor compared to active state (3,305 ± 691.2 copies per million in active; 19,850 ± 6,292 copies per million in torpor; p = 0.02, Tukey's multiple comparisons test; Figure 3C). Together, these results demonstrate that antidiuretic hormone transcripts are abundant in the SON during torpor, in agreement with the observations of the rapid mobilization of DCVs and the increase in plasma OXT and AVP during the early stages of the torpor-arousal transition.

To assess whether SON neurons are translationally active during the torpor-arousal transition, we performed immunohistochemistry (IHC) for the protein product of the immediate early

Please cite this article in press as: Junkins et al., Neural control of fluid homeostasis is engaged below 10°C in hibernation, Current Biology (2024), https://doi.org/10.1016/j.cub.2024.01.035

gene c-FOS. Although antibodies against OXT did not work in squirrel tissues, we successfully performed co-staining for AVP and c-FOS. Strikingly, the abundance of translationally active (c-FOS$^+$) AVP$^+$ neurons was the highest during torpor (29.07% ± 3.28%) and early arousal at 10°C (27.23% ± 3.86%), a nearly 6-fold increase over the abundance of such neurons in IBA (4.4% ± 0.83%; torpor vs. IBA, $p = 0.0033$; 10°C vs. IBA, $p = 0.0064$, Tukey's multiple comparisons test, Figures 3D and 3E). These results provide neuroanatomical evidence supporting the hypothesis that AVP neurons are translationally active at temperatures as low as 10°C during the torpor-arousal transition.

Dynamic *in vivo* hypothalamic neuronal activity at 10°C

Vasopressinergic and oxytocinergic magnocellular neurons in the SON are intrinsically osmosensitive, firing action potentials in a manner that tracks increases in serum osmolality and triggering the release of their respective antidiuretic hormones into circulation.[8] Furthermore, SON neurons receive feedforward information from the lamina terminalis and change firing activity to anticipate and combat future changes in systemic osmolality.[17,18] Our observations of DCV dynamics, hormonal release, and c-FOS expression suggest that SON neurons are active at low T_B during the torpor-arousal transition. To test this hypothesis, we used *in vivo* fiber photometry to monitor the activity of AAV9-CaMKII-GCaMP6s-expressing SON neurons during arousal (Figure 4A). This experiment allowed us to observe population neuronal dynamics in an unbiased manner across the torpor-arousal transition to pinpoint the lowest temperature at which neural activity occurs. In seven squirrels with viral expression that colocalized with SON^{AVP} neurons, GCaMP6s signal began to change dynamically at low temperatures and continued to increase until T_B reached homeothermic levels (Figures 4B, lower panel, and S1). For example, one animal first exhibited an increase in GCaMP6s signal around 1,400 s into the recording, at $T_B \sim 6$°C (Figure 4B, upper panel, colocalization of GCaMP and AVP for this animal shown in Figure 4C). The averaged GCaMP6s fluorescence began to increase at ~1,300 s into the recording, when the average T_B reached 6°C (Figure 4B, lower panel).

Next, we used the same cohort of animals to ask whether the responding SON neurons are sensitive to acute increases in blood osmolality during the early stages of the torpor-arousal transition. Intraperitoneal injection of 2 M NaCl stimulated GCaMP6s fluorescence, which increased in the first 6 min of arousal even before T_B of all animals surpassed 4°C–5°C (Figure 4D). This effect was dose-dependent and specific, as the injection of 3 M NaCl stimulated fluorescence further, while no increase was observed without the hypertonic injection (Figure 4D) or in an animal whose hypothalamic viral expression that did not colocalize with SON^{AVP} neurons (Figure S2). There was a significant fixed effect of treatment ($p < 0.0001$; linear mixed model) and a significant difference in all pairwise comparisons ($p < 0.0001$; Tukey's multiple comparisons test) (Figure 4D). These results demonstrate that osmosensitive SON neurons are functional during early arousal and respond to perturbations of fluid homeostasis, when T_B is as low as 5°C.

Conclusions

The maintenance of existing body fluid levels is a particularly urgent matter for 13LGS, which undergo up to 30 torpor-arousal cycles throughout a hibernation season.[1,6] The torpor-arousal transition, during which blood osmolality and blood pressure both rise precipitously,[1,12,13] could lead to excessive diuresis without the timely release of antidiuretic hormones.[19] In this study, we have demonstrated that the hypothalamic-pituitary axis is functional by the time T_B of arousing squirrels reaches 10°C. Dynamic changes in plasma levels of OXT and AVP, posterior pituitary function, and SON neuron activity all underscore the remarkable activation of this pathway under cold internal temperatures.

Here, we focused on the SON, whose singular known role is the production and release of AVP and OXT. However, a similar role is also played by a subset of neurons in the functionally diverse PVH region.[20] Future studies should address the relationship between AVP$^+$ and OXT$^+$ neurons in SON and PVH during the torpor-arousal transition and the extent to which their roles are functionally redundant.

We observed that the SON accumulates *Avp* and *Oxt1/2* transcripts during torpor, in agreement with observations of the expression of various neuronal genes during torpor in 13LGS.[21] This suggests that either gene transcription occurs at T_B close to 4°C or during late IBA just prior to torpor. Further research is necessary to distinguish between these possibilities. In any case, neuronal genes undergo RNA processing during torpor, potentially stabilizing them for long-term storage.[22,23] It has long been established that the antidiuretic hormones are stored in hypothalamic cell bodies and the posterior pituitary during hibernation in several species.[24–27] Here, we determined that the release of AVP and OXT from DCVs in the posterior pituitary into circulation is underway by the time the arousing squirrel reaches 10°C, enabling water retention throughout the torpor-arousal transition.

Previous work has shown c-FOS expression in various brain regions of several hibernating species across physiological states.[28–32] Arctic ground squirrels show a 23% increase in c-FOS$^+$ SON neurons during IBA compared to active state,[33] but the function of this expression remained unclear. SON^{AVP} neurons have a well-established role in fluid homeostasis by releasing AVP via the posterior pituitary. Our observation that the abundance of c-FOS$^+$ neurons within the AVP$^+$ SON population peaks during torpor and 10°C, links SON neural activity to hormone release at the early stages of arousal.

Our fiber photometry experiments tracked hypothalamic neuronal activity for the duration of the torpor-arousal transition (Figures 4B and 4D). It is important to note that the population of neurons we recorded from included SON^{AVP} neurons, as confirmed by IHC, but also included other hypothalamic neurons (Figures 4C and S1). In one squirrel, who did not show colocalization of GCaMP6s with AVP, there was still a similar pattern of fluorescence across the torpor-arousal transition but without any osmosensory activity (Figure S2). We propose that activity must originate at low temperatures in other hypothalamic regions to support several homeostatic processes across the torpor-arousal transition, such as thermogenesis.[7]

One limitation of our study is that because of the absence of AVP- or OXT-specific promoters validated in ground squirrels, we had to rely on the CaMKII promoter to drive GCaMP6s expression in excitatory neurons in the vicinity of the injection site. Nonetheless, we confirmed that our recordings included

Please cite this article in press as: Junkins et al., Neural control of fluid homeostasis is engaged below 10°C in hibernation, Current Biology (2024), https://doi.org/10.1016/j.cub.2024.01.035

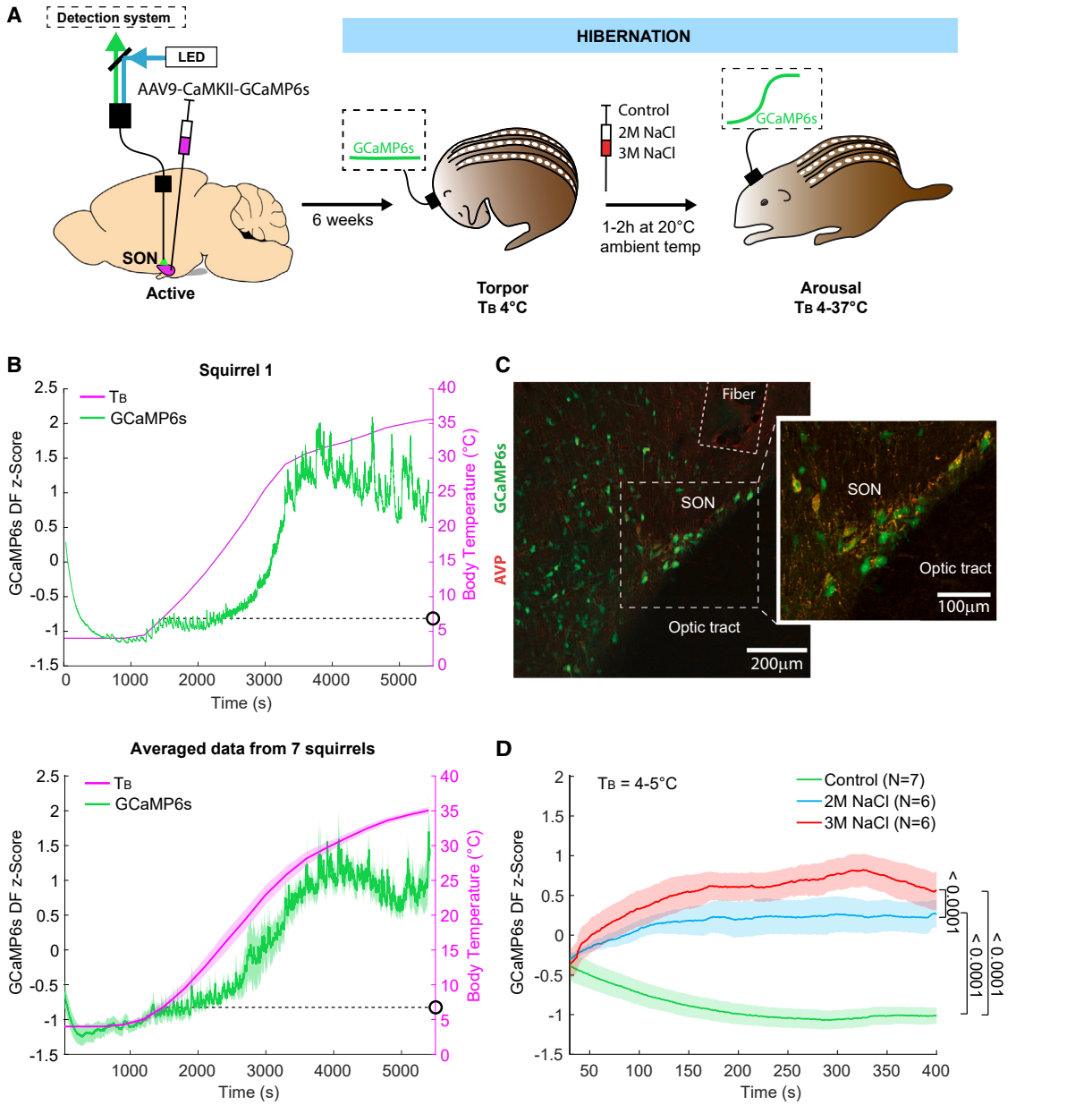

Figure 4. Osmosensitive SON neurons are functional at low temperature during early arousal

(A) Experimental setup for *in vivo* monitoring of GCaMP6s fluorescence in SON neurons.

(B) Continuous recording of GCaMP6s fluorescence in SON (green, left axis) and corresponding T_B (pink, right axis) during arousal in one representative animal (upper) and averaged data from seven animals, shown as mean ± SEM (lower).

(C) Image showing AVP-expressing cells (immunostaining; red), GCaMP6s-epxressing cells (native fluorescence; green), and the position of the optical fiber above SON of squirrel 1, corresponding to the data presented in (B). Inset shows a high magnification image of the area outlined by the dotted white line containing AVP^+ SON neurons.

(D) Osmolality-dependent increase of GCaMP6s signal in SON at body temperature of 4°C–5°C during the first 400 s of recording in response to intraperitoneal injection of 2 or 3 M NaCl, shown as mean ± SEM. Control (n = 7), 2 M NaCl (n = 6), 3 M NaCl (n = 6). Linear mixed model: a significant fixed effect of treatment ($p < 0.0001$). Numbers on the side denote p values from Tukey's multiple comparisons test.

See also Figures S1 and S2.

SON neurons by leveraging their unique osmosensitive properties: by injecting squirrels with 2 and 3 M NaCl, we ascertained that osmosensitive SON neurons can be activated in a dose-dependent manner even before squirrels reach 5°C during early arousal.

In vitro, the minimum temperature permissible for activity in neurons from mammalian non-hibernators is 15°C, whereas neurons from hibernators can fire at even lower temperatures.[34] However, few studies of neural activity have been performed *in vivo* during hibernation.[35] Electrophysiological experiments

Please cite this article in press as: Junkins et al., Neural control of fluid homeostasis is engaged below 10°C in hibernation, Current Biology (2024), https://doi.org/10.1016/j.cub.2024.01.035

CellPress

have revealed almost no electrical signal in the cortex or thalamus during torpor.[36–38] Although external sensory stimuli can elicit responses in the brainstem and cortex at just above 9°C,[36,39,40] there has been no evidence of hypothalamic neuronal activity during the torpor-arousal transition for the purposes of interoception and homeostasis. Here we show, using fiber photometry for the first time in an obligatory hibernator, that neural activity can occur even below 10°C during the torpor-arousal transition in response to an acute increase in blood osmolality. In sum, the activity of osmosensitive SON neurons allows for the release of AVP and OXT from DCVs in the posterior pituitary into the circulation by 10°C to promote water retention as animals arouse from torpor.

STAR★METHODS

Detailed methods are provided in the online version of this paper and include the following:

- KEY RESOURCES TABLE
- RESOURCE AVAILABILITY
  - Lead contact
  - Materials availability
  - Data and code availability
- EXPERIMENTAL MODEL AND SUBJECT DETAILS
- METHOD DETAILS
  - Arousal from torpor
  - Serum, plasma, and pituitary collection
  - Plasma vasopressin and oxytocin measurement
  - Pituitary vasopressin/oxytocin measurement
  - Electron microscopy
  - RNA isolation and sequencing
  - Immunohistochemistry (IHC)
  - Stereotaxic surgery
  - Fiber photometry
  - Data analysis for fiber photometry
- QUANTIFICATION AND STATISTICAL ANALYSES

SUPPLEMENTAL INFORMATION

Supplemental information can be found online at https://doi.org/10.1016/j.cub.2024.01.035.

ACKNOWLEDGMENTS

We thank Sue Ann Mentone for assistance in tissue processing and electron microscopy, Sarah Mohr and Viktor Feketa for assistance with transcriptome analysis, and members of the Gracheva and Bagriantsev laboratories for their comments throughout the project. The graphical abstract was created with BioRender.com. This study was funded by the Warren Alpert Distinguished Scholar Award to N.Y.F., Axle Tech International Endowed Professorship to D.K.M., NSF grants IOS-1754286 and IOS-2015622 to E.O.G., and NIH grant R01NS126271 to E.O.G.

AUTHOR CONTRIBUTIONS

N.Y.F., M.S.J., S.N.B., and E.O.G. conceptualized the study. N.Y.F., M.S.J., and L.A.M. performed experiments and collected and analyzed data. G.C. contributed to fiber photometry data analysis. D.K.M. supplied squirrels and advised on animal husbandry. M.S.J., N.Y.F., S.N.B., and E.O.G. wrote the manuscript, with contributions from L.A.M. and D.K.M. S.N.B. and E.O.G. provided guidance and supervision.

DECLARATION OF INTERESTS

The authors declare no competing interests.

Received: May 14, 2023
Revised: November 29, 2023
Accepted: January 12, 2024
Published: February 6, 2024

REFERENCES

1. Feng, N.Y., Junkins, M.S., Merriman, D.K., Bagriantsev, S.N., and Gracheva, E.O. (2019). Osmolyte Depletion and Thirst Suppression Allow Hibernators to Survive for Months without Water. Curr. Biol. *29*, 3053–3058.e3.
2. Mohr, S.M., Bagriantsev, S.N., and Gracheva, E.O. (2020). Cellular, Molecular, and Physiological Adaptations of Hibernation: The Solution to Environmental Challenges. Annu. Rev. Cell Dev. Biol. *36*, 315–338.
3. Andrews, M.T. (2019). Molecular interactions underpinning the phenotype of hibernation in mammals. J. Exp. Biol. *222*, jeb160606.
4. Carey, H.V., Andrews, M.T., and Martin, S.L. (2003). Mammalian hibernation: cellular and molecular responses to depressed metabolism and low temperature. Physiol. Rev. *83*, 1153–1181.
5. Ruf, T., and Geiser, F. (2015). Daily torpor and hibernation in birds and mammals. Biol. Rev. Camb. Philos. Soc. *90*, 891–926.
6. Dai Pra, R., Mohr, S.M., Merriman, D.K., Bagriantsev, S.N., and Gracheva, E.O. (2022). Ground squirrels initiate sexual maturation during hibernation. Curr. Biol. *32*, 1822–1828.e4.
7. Junkins, M.S., Bagriantsev, S.N., and Gracheva, E.O. (2022). Towards understanding the neural origins of hibernation. J. Exp. Biol. *225*, jeb229542.
8. Bourque, C.W. (2008). Central mechanisms of osmosensation and systemic osmoregulation. Nat. Rev. Neurosci. *9*, 519–531.
9. Zimmerman, C.A., Leib, D.E., and Knight, Z.A. (2017). Neural circuits underlying thirst and fluid homeostasis. Nat. Rev. Neurosci. *18*, 459–469.
10. Leib, D.E., Zimmerman, C.A., and Knight, Z.A. (2016). Thirst. Curr. Biol. *26*, R1260–R1265.
11. Augustine, V., Lee, S., and Oka, Y. (2020). Neural Control and Modulation of Thirst, Sodium Appetite, and Hunger. Cell *180*, 25–32.
12. Lyman, C.P., and O'Brien, R.C. (1961). Circulatory changes in the 13-lined ground squirrel during the hibernating cycle. Tech. Rep. Arct. Aeromed. Lab. US *60*, 1–18.
13. Horwitz, B.A., Chau, S.M., Hamilton, J.S., Song, C., Gorgone, J., Saenz, M., Horowitz, J.M., and Chen, C.Y. (2013). Temporal relationships of blood pressure, heart rate, baroreflex function, and body temperature change over a hibernation bout in Syrian hamsters. Am. J. Physiol. Regul. Integr. Comp. Physiol. *305*, R759–R768.
14. Goodson, J.L. (2008). Nonapeptides and the evolutionary patterning of sociality. Prog. Brain Res. *170*, 3–15.
15. Li, C., Wang, W., Summer, S.N., Westfall, T.D., Brooks, D.P., Falk, S., and Schrier, R.W. (2008). Molecular mechanisms of antidiuretic effect of oxytocin. J. Am. Soc. Nephrol. *19*, 225–232.
16. Morris, J.F. (2020). Neurosecretory Vesicles: Structure, Distribution, Release and Breakdown. In Neurosecretion: Secretory Mechanisms, J.R. Lemos, and G. Dayanithi, eds. (Springer International Publishing), pp. 81–102.
17. Mandelblat-Cerf, Y., Kim, A., Burgess, C.R., Subramanian, S., Tannous, B.A., Lowell, B.B., and Andermann, M.L. (2017). Bidirectional Anticipation of Future Osmotic Challenges by Vasopressin Neurons. Neuron *93*, 57–65.
18. Kim, A., Madara, J.C., Wu, C., Andermann, M.L., and Lowell, B.B. (2021). Neural basis for regulation of vasopressin secretion by anticipated disturbances in osmolality. eLife *10*, e66609.

Please cite this article in press as: Junkins et al., Neural control of fluid homeostasis is engaged below 10°C in hibernation, Current Biology (2024), https://doi.org/10.1016/j.cub.2024.01.035

19. Christ-Crain, M., Bichet, D.G., Fenske, W.K., Goldman, M.B., Rittig, S., Verbalis, J.G., and Verkman, A.S. (2019). Diabetes insipidus. Nat. Rev. Dis. Primers *5*, 54.
20. Xu, S., Yang, H., Menon, V., Lemire, A.L., Wang, L., Henry, F.E., Turaga, S.C., and Sternson, S.M. (2020). Behavioral state coding by molecularly defined paraventricular hypothalamic cell type ensembles. Science *370*, eabb2494.
21. Schwartz, C., Hampton, M., and Andrews, M.T. (2013). Seasonal and regional differences in gene expression in the brain of a hibernating mammal. PLoS One *8*, e58427.
22. Fu, R., Gillen, A.E., Grabek, K.R., Riemondy, K.A., Epperson, L.E., Bustamante, C.D., Hesselberth, J.R., and Martin, S.L. (2020). Dynamic RNA Regulation in the Brain Underlies Physiological Plasticity in a Hibernating Mammal. Front. Physiol. *11*, 624677.
23. Riemondy, K.A., Gillen, A.E., White, E.A., Bogren, L.K., Hesselberth, J.R., and Martin, S.L. (2018). Dynamic temperature-sensitive A-to-I RNA editing in the brain of a heterothermic mammal during hibernation. RNA *24*, 1481–1495.
24. Hudson, J.W., and Wang, L.C.H. (1979). Hibernation: Endocrinologic Aspects. Annu. Rev. Physiol. *41*, 287–303.
25. Jasiński, A. (1970). Hypothalamic Neurosecretion in the Bat, Myotis myotis Borkhausen, during the Period of Hibernation and Activity. Held in Berlin, Heidelberg (Springer), pp. 301–309.
26. Yurisova, M.N., and Polenov, A.L. (1979). The hypothalamo-hypophysial system in the ground squirrel, Citellus erythrogenys Brandt. II. Seasonal changes in the classical neurosecretory system of a hibernator. Cell Tissue Res. *198*, 539–556.
27. Theodosis, D.T., Burlet, C., Boudier, J.L., and Dreifuss, J.J. (1978). Morphology of membrane changes during neurohypophyseal hormone release in a hibernating rodent. Brain Res. *154*, 371–376.
28. Ikeno, T., Williams, C.T., Buck, C.L., Barnes, B.M., and Yan, L. (2017). Clock Gene Expression in the Suprachiasmatic Nucleus of Hibernating Arctic Ground Squirrels. J. Biol. Rhythms *32*, 246–256.
29. Bratincsák, A., McMullen, D., Miyake, S., Tóth, Z.E., Hallenbeck, J.M., and Palkovits, M. (2007). Spatial and temporal activation of brain regions in hibernation: c-fos expression during the hibernation bout in thirteen-lined ground squirrel. J. Comp. Neurol. *505*, 443–458.
30. El Quezzani, S., Tramu, G., and Magoul, R. (1999). Neuronal activity in the mediobasal hypothalamus of hibernating jerboas (Jaculus orientalis). Neurosci. Lett. *260*, 13–16.
31. O'Hara, B.F., Watson, F.L., Srere, H.K., Kumar, H., Wiler, S.W., Welch, S.K., Bitting, L., Heller, H.C., and Kilduff, T.S. (1999). Gene expression in the brain across the hibernation cycle. J. Neurosci. *19*, 3781–3790.
32. Bitting, L., Sutin, E.L., Watson, F.L., Leard, L.E., O'Hara, B.F., Heller, H.C., and Kilduff, T.S. (1994). C-fos mRNA increases in the ground squirrel suprachiasmatic nucleus during arousal from hibernation. Neurosci. Lett. *165*, 117–121.
33. Frare, C., Jenkins, M.E., McClure, K.M., and Drew, K.L. (2019). Seasonal decrease in thermogenesis and increase in vasoconstriction explain seasonal response to N(6) -cyclohexyladenosine-induced hibernation in the Arctic ground squirrel (Urocitellus parryii). J. Neurochem. *151*, 316–335.
34. Chatfield, P.O., and Battista, A.F. (1948). Effects of cooling on nerve conduction in a hibernator, golden hamster, and non-hibernator, albino rat. Am. J. Physiol. *155*, 179–185.
35. Sonntag, M., and Arendt, T. (2019). Neuronal Activity in the Hibernating Brain. Front. Neuroanat. *13*, 71.
36. Chatfield, P.O., Lyman, C.P., and Purpura, D.P. (1951). The effects of temperature on the spontaneous and induced electrical activity in the cerebral cortex of the golden hamster. Electroencephalogr. Clin. Neurophysiol. *3*, 225–230.
37. Andersen, P., Johansen, K., and Krog, J. (1960). Electroencephalogram during arousal from hibernation in the birchmouse. Am. J. Physiol. *199*, 535–538.
38. Krilowicz, B.L., Glotzbach, S.F., and Heller, H.C. (1988). Neuronal activity during sleep and complete bouts of hibernation. Am. J. Physiol. *255*, R1008–R1019.
39. Strumwasser, F. (1959). Regulatory mechanisms, brain activity and behavior during deep hibernation in the squirrel, Citellus beecheyi. Am. J. Physiol. *196*, 23–30.
40. Hamill, N.J., McGinn, M.D., and Horowitz, J.M. (1989). Auditory brainstem responses in ground squirrels arousing from hibernation. J. Comp. Physiol. B *159*, 167–172.
41. Robinson, M.D., McCarthy, D.J., and Smyth, G.K. (2010). edgeR: a Bioconductor package for differential expression analysis of digital gene expression data. Bioinformatics *26*, 139–140.
42. Schindelin, J., Arganda-Carreras, I., Frise, E., Kaynig, V., Longair, M., Pietzsch, T., Preibisch, S., Rueden, C., Saalfeld, S., Schmid, B., et al. (2012). Fiji: an open-source platform for biological-image analysis. Nat. Methods *9*, 676–682.
43. Laursen, W.J., Mastrotto, M., Pesta, D., Funk, O.H., Goodman, J.B., Merriman, D.K., Ingolia, N., Shulman, G.I., Bagriantsev, S.N., and Gracheva, E.O. (2015). Neuronal UCP1 expression suggests a mechanism for local thermogenesis during hibernation. Proc. Natl. Acad. Sci. USA *112*, 1607–1612.
44. Schwartz, C., Hampton, M., and Andrews, M.T. (2015). Hypothalamic gene expression underlying pre-hibernation satiety. Genes Brain Behav. *14*, 310–318.
45. Mohr, S.M., Pra, R.D., Platt, M.P., Feketa, V.V., Shanabrough, M., Varela, L., Kristant, A., Cao, H., Merriman, D.K., Horvath, T.L., et al. (2023). Hypothalamic thyroid hormone deficiency underlies reversible anorexia in a mammalian hibernator. https://doi.org/10.1101/2023.03.15.532843.
46. Paxinos, G., and Franklin, K.B.J. (2013). The Rat Brain in Stereotaxic Coordinates, Seventh Edition (Elsevier).
47. Zimmerman, C.A., Lin, Y.C., Leib, D.E., Guo, L., Huey, E.L., Daly, G.E., Chen, Y., and Knight, Z.A. (2016). Thirst neurons anticipate the homeostatic consequences of eating and drinking. Nature *537*, 680–684.

Please cite this article in press as: Junkins et al., Neural control of fluid homeostasis is engaged below 10°C in hibernation, Current Biology (2024), https://doi.org/10.1016/j.cub.2024.01.035

CellPress

STAR★METHODS

KEY RESOURCES TABLE

REAGENT or RESOURCE	SOURCE	IDENTIFIER
Antibodies		
Mouse anti-cfos	Santa Cruz Biotechnology	Cat# sc-271243; RRID:AB_10610067
Rabbit anti-avp	Millipore Sigma	Cat# AB1565; RRID: AB_90782
Alexa Fluor goat anti-mouse 488	Thermo Fisher	Cat# A1101; RRID:AB_2534069
Alexa Fluor goat anti-rabbit 555	Abcam	Cat# ab150086; RRID:AB_2890032
Bacterial and virus strains		
AAV9.CaMKII.GCaMP6s.WPRE.SV40	Addgene; gift from James M. Wilson	Cat# 107790; RRID:Addgene_107790
Critical commercial assays		
Oxytocin ELISA kit	Enzo Life Sciences	Cat# ADI-901-153A
Vasopressin ELISA kit	Enzo Life Sciences	Cat# ADI-900-017A
Quick-RNA Microprep Kit	Zymo	Cat# R1050
Deposited data		
Raw and analyzed bulk RNA-Seq data for Squirrel SON	This paper	GEO: GSE231418
SpeTri2.0 Reference Genome	Broad Institute	NCBI: GCA_000236235.1
Experimental models: Organisms/strains		
Thirteen-lined ground squirrel: *Ictidomys tridecemlineatus*	University of Wisconsin Oshkosh	N/A
Software and algorithms		
Prism version 10.0	GraphPad	RRID:SCR_002798
MATLAB version R2023a	MathWorks	RRID:SCR_001622
TDTbin2mat function	Tucker-Davis Technologies	https://www.tdt.com/docs/sdk/offline-data-analysis/offline-data-matlab/#tdtbin2mat
R Project for Statistical Computing version 4.0.2	R Project for Statistical Computing	RRID:SCR_001905
EdgeR version 3.30.3	Bioconductor.org; Robinson et al.[41]	RRID:SCR_012802
FIJI version 1.0	Fiji; Schindelin et al.[42]	RRID:SCR_002285
Synapse version 96	Tucker-Davis Technologies	https://www.tdt.com/component/synapse-software/
Other		
IPTT-300 Temperature Transponder	Bio Medic Data Systems	IPTT-300
OsmoTECH Osmometer	Advanced Instruments	https://www.aicompanies.com/bioprocessing-osmometers/osmotech-single-sample-micro-osmometer/
Spectramax 384 Plus plate reader	Molecular Devices	www.moleculardevides.com
BioAnalyzer 2100	Agilent Technologies	RRID:SCR_019715
Model 940 Small Animal Stereotaxic Instrument	Kopf Instruments	https://kopfinstruments.com/product/model-940-small-animal-stereotaxic-instrument-with-digital-display-console/
Nanoject III Programmable Nanoliter Injector	Drummond Scientific	Cat# 3-000-207
Fiber Optic Cannula	Doric	MFC_400/430-0.66_10mm_MF2.5_FLT
RZ10x Expanded Lux10 Processor	Tucker-Davis Technologies	https://www.tdt.com/component/rz10x-processor/

Please cite this article in press as: Junkins et al., Neural control of fluid homeostasis is engaged below 10°C in hibernation, Current Biology (2024), https://doi.org/10.1016/j.cub.2024.01.035

RESOURCE AVAILABILITY

Lead contact

Further information and requests for resources and reagents should be directed to and will be fulfilled by the lead contact, Elena Gracheva (elena.gracheva@yale.edu).

Materials availability

This study did not generate new unique reagents.

Data and code availability

- RNA sequencing data are deposited to the Gene Expression Omnibus, accession number GSE231418, and are publicly available as of the date of publication.
- All other data reported in this paper will be shared by the lead contact upon request.
- This paper does not report original code.

EXPERIMENTAL MODEL AND SUBJECT DETAILS

Thirteen-lined ground squirrels were housed in temperature and humidity-controlled facilities at Yale University. During the active season (Summer-Fall), animals were held in a vivarium with room temperature of 18-20°C, a photoperiod of 12h:12h light:dark, and maintained on a diet of dog food (Iams) supplemented with sunflower seeds, superworms, and fresh vegetables, with ad libitum access to water. During the hibernation season, animals who recently experienced hypothermic bouts were moved to a hibernaculum with 2-4°C room temperature, constant darkness, 40%–60% humidity, and no access to food or water. Squirrels entered torpor within 1-3 days of being moved to the hibernaculum. All squirrels were implanted with an intrascapular temperature transponder (BMDS, LLC) and temperature was measured using a remote reader every day to track hibernation states. Although only T_B was measured for this study, brain temperature closely tracks T_B in thirteen-lined ground squirrels.[43] In this study, ''active'' squirrels were those who held a constant body temperature (T_B) of 37°C while being kept in the vivarium, torpor squirrels were those whose T_B in the hibernaculum remained below 5°C, while IBA squirrels were those whose T_B in the hibernaculum remained above 35°C for at least 1.5 h following a torpor bout. Active squirrels were collected from June to October, never experienced hypothermic bouts and did not include fall-active animals[44]; hibernating squirrels (including torpor, arousal, and IBA) were collected throughout the entire hibernation season, from August to March, because the maintenance of fluid homeostasis is critical during early and late hibernation. Prior to use, hibernating animals experienced a minimum of 2 and a maximum of 28 torpor bouts (mean = 10.65 ± 0.58 SEM), with a minimum of 2 and a maximum of 26 days in torpor since the previous IBA (mean = 6.825 ± 0.46 SEM). Both males and females (aged 9 months – 3 years) were used in these studies and combined in analyses as fluid homeostasis is essential for the basic survival of both sexes. Numbers of males and females for each experiment are reported in Table S1. All animal procedures were performed in compliance with the Office of Animal Research Support of Yale University (protocol 2021-11497).

METHOD DETAILS

Arousal from torpor

Torpid animals (T_B = 4°C) were brought from the hibernaculum into the well-lit laboratory at room temperature. Animals were then allowed to arouse in their cage without being handled to one of several points before tissue collection: 10°C (early transition stage), 27°C (late transition stage for ELISA and IHC experiments), or 32°C (late transition stage for electron microscopy experiments).

Serum, plasma, and pituitary collection

Animals were euthanized by isoflurane overdose. 2 to 4 mL of blood was first collected by cardiac puncture into K2 EDTA tubes (Fisher Scientific, Waltham, MA), with 50 μL of 5 mg/mL aprotinin (Sigma). Plasma was collected by spinning at 4°C for 15 min at 1600 g, supernatant removed, and flash frozen on dry ice, and stored in -80°C until use for hormone measurement. The remaining blood was collected and allowed to coagulate at room temperature for 30 min before spinning at 4°C for 15 min at 2000 g. Serum was removed, 20 μL was used for measurement of osmolality on an OsmoTECH Osmometer (Advanced Instruments, Norwood, MA). The pituitary was removed with fine forceps under a light microscope from the base of the skull after removing the rest of the brain and stored in Eppendorf tubes at -80°C until use.

Plasma vasopressin and oxytocin measurement

Plasma vasopressin (AVP) and oxytocin (OXT) levels were measured with enzyme linked immunoassay (ELISA) kits (Enzo Life Sciences, Inc., Farmingdale, NY) as previously described.[1] 500 μL of plasma from each animal was extracted using 100 mg C18 Sep-Pak columns (Waters Corporation, Milford, MA) on a vacuum manifold (Waters Corporation). Briefly, plasma was thawed on ice, combined with 500 mL 1% Trifluoroacetic acid (TFA), and centrifuged at 4°C for 20 min at a maximum speed of 15,000 rpm.

Please cite this article in press as: Junkins et al., Neural control of fluid homeostasis is engaged below 10°C in hibernation, Current Biology (2024), https://doi.org/10.1016/j.cub.2024.01.035

Columns were activated with 500 μL methanol and washed three times with 1 mL 1% TFA. 1 mL of the spun plasma sample was loaded into columns and flowed through slowly over 2 min. The OXT fraction was eluted and collected with 3 mL of 98% acetone, then the AVP fraction was eluted and collected with 3 mL of 80% acetonitrile containing 0.1% TFA (v/v). Collected fractions were evaporated to dryness under nitrogen. For AVP ELISA, 500 mL of the assay buffer was added to the dried fraction and the rest of the assay followed the manufacturer's instructions. For OXT ELISA, the dried fraction was either stored at -20°C until use or assayed immediately following manufacturer's instructions.

All standards and samples were run in duplicate. Optical density at assay-specific wavelengths were read by a Spectramax 384 Plus plate reader (Molecular Devices). The standard curves were fit with 4-parameter logistic regression in GraphPad Prism 10.0 (GraphPad Software). Values above the standard curve limit were assigned the maximum value (1000 pg/mL). The samples that were below the detection limit of the assay were assigned a value of 7.5 pg/ml for OXT and 1.42 pg/ml for AVP (1/2 of the manufacturer's reported detection limit). A non-parametric Kruskal-Wallis test followed by Dunn's multiple comparisons test was performed using GraphPad Prism 10.0 to assess state-dependent differences in AVP and OXT.

Pituitary vasopressin/oxytocin measurement

Pituitary AVP and OXT levels were measured as previously described.[1] To extract and measure AVP and OXT from the pituitary, 200 μL of the appropriate ELISA assay buffer and 20 μL of 5mg/mL aprotinin were added to each tube, and the pituitary was mechanically dissociated on ice using a pestle (Corning Inc., Corning, NY). The rest of the assay followed the manufacturer's instructions. For OXT, the initial dissociated pituitary was diluted 10,000 times in assay buffer to stay within assay detection limits since pituitary OXT content is extremely high. One-way ANOVA with Tukey's multiple comparisons test was performed using GraphPad Prism 10.0 to assess state-dependent differences in pituitary AVP and OXT content.

Electron microscopy

Animals were sacrificed by isoflurane gas overdose and decapitated. After trunk blood was removed, the pituitary was removed from the base of the skull with fine forceps and fixed in 0.1% tannic acid and 2% glutaraldehyde in 0.1M cacodylate buffer at 4°C on a rocking platform for 2 h. The pituitary was then held in 0.1M Cacodylate Buffer and rocked overnight at 4°C. The following day, the pituitary was post-fixed with Palade's osmium (pH 7.6) for 1 h at 4°C in the dark. After washing with 0.1M Na^+ cacodylate buffer (pH 7.4), the pituitary was then stained in Kellenburger solution containing 0.5% wt/vol Uranyl acetate (pH 6.0) for 1 h at room temperature. After washing with double distilled H2O, the pituitary was dehydrated through increasing concentrations of ethanol (40%, 60%, 70%, 80%, and 96%, 10 min each) and then in 100% acetone (three changes, 10 min each). The pituitary was embedded in 50/50 acetone/EMbed 812 resin (Electron Microscopy Services) for 2 h, and then twice in 100% EMbed 812 for 1 h. Ultra-thin sections (800Å) were cut and placed on copper grids, then coated with 0.8% Pioloform solution. Finally, the grids were stained with 1.5% aqueous Uranyl acetate and Reynolds Lead Citrate solution.

Electron micrographs of pituitaries were obtained on a Tecnai G2 Spirit BioTWIN (LaB6, 80 kV) at magnifications of 9,900 – 26,500x to accommodate variation in axon ending size. Images were analyzed with ImageJ. Briefly, neurosecretory axon endings were identified by the presence of both large dense core vesicles (DCVs) known to contain either AVP or OXT as well as small clear vesicles known to contain glutamate.[16] Clear-core vesicles were used to identify neurosecretory endings but were not measured in this study. The area of the axon endings and number of DCVs were counted with the Cell Counter plugin. The density of DCVs (number of DCVs/area in μm^2) was computed in Excel.

RNA isolation and sequencing

Bulk RNA Sequencing was performed as previously described.[45] Total RNA was isolated from the supraoptic nuclei of active (n = 5), torpid (n=5), and IBA (n = 5) animals that had been deeply anesthetized by isoflurane inhalation and subjected to intracardiac perfusion with ice-cold PBS. The brain was rapidly dissected and a vibratome (Leica VT1200) was used to cut 300–600 μm coronal slices. Slices containing the supraoptic nucleus were identified using the optic chiasm as a landmark.[33,46] The supraoptic nucleus was manually dissected out from the slices using 27G needles and placed immediately into RNA lysis buffer from the Quick-RNA Microprep Kit (Zymo, R1050). Total RNA was isolated from tissue using the Quick-RNA Microprep Kit (Zymo, R1050). RNA concentration and integrity number (RIN) were assessed by an Agilent 2100 Bioanalyzer (Agilent, Santa Clara, CA). RNA concentrations were in the range of ~5 – 42 ng/μL (mean 23 ng/μL) and RIN values were in the range of 7.3 – 8.8 (mean 8.0).

Library preparation and sequencing were carried out at the Yale Center for Genome Analysis. Sequencing libraries were prepared using the Kapa mRNA Hyper Prep Kit (Cat# KR1352, Roche) including rRNA depletion. Libraries were sequenced on the Illumina NovaSeq6000 in the 100 bp paired-end mode according to manufacturer's protocols. A total of 39.8 – 57.1 million sequencing read pairs (mean 48.5 million read pairs) per sample were obtained.

The sequencing data were processed on the Yale Center for Research Computing cluster. Raw sequencing reads were filtered and trimmed to retain high-quality reads using Trimmomatic v0.39 with default parameters. Filtered high-quality reads from all samples were aligned to the *Ictidomys tridecemlineatus* reference genome using the STAR aligner v2.7.1a with default parameters. We obtained 64.85% ± 0.8% (mean ± standard error of the mean) of uniquely mapped reads. The SpeTri2.0 [GCA_000236235.1] reference genome and the gene annotation were obtained from the Broad Institute. The gene annotation was filtered to include only protein-coding genes. Aligned reads were counted by the featureCounts programs from the Subread package v2.2.0 with default parameters. Read counting was performed at the gene level, i.e., the final read count for each gene included all reads mapped to all exons of

Please cite this article in press as: Junkins et al., Neural control of fluid homeostasis is engaged below 10°C in hibernation, Current Biology (2024), https://doi.org/10.1016/j.cub.2024.01.035

this gene. We obtained a list of differential expression of genes by performing EdgeR v 3.30.3[41] with the GLM approach and quasi-likelihood F-test and using a significance value of FDR <0.05. Normalized read counts were obtained by normalizing raw read counts to effective library sizes of each sample and expressed as counts per million of total reads in a library (CPM).

The NCBI gene symbol LOC101970427 refers to ''vasopressin-neurophysin 2-copeptin-like [Ictidomys tridecemlineatus]'', which we designated as *Avp*. The gene ID LOC101967926 refers to ''oxytocin-neurophysin 1 [Ictidomys tridecemlineatus]'', which we designated as *Oxt1*. The gene symbol LOC101967640 also refers to ''oxytocin-neurophysin 1 [Ictidomys tridecemlineatus]'', which we designated as *Oxt2*. Transcript CPM were plotted in GraphPad Prism 10.0 (GraphPad Software) and an ordinary one-way ANOVA with Tukey's multiple comparisons test was performed on the data. *Avp* expression levels were significantly different across states as determined by EdgeR and one-way ANOVA, so we reported both FDR value as well as the post-hoc Tukey's multiple comparisons in Figure 3C.

RNA sequencing data (Data S1) are deposited to the Gene Expression Omnibus, accession number GSE231418.

Immunohistochemistry (IHC)

Animals were anesthetized by isoflurane overdose and intracardially perfused with ice-cold 30 mL PBS (1x PBS, Teknova) followed by 30 mL of ice-cold 4% paraformaldehyde (PFA; ChemCruz). Brains were postfixed in 4% PFA at 4°C overnight, then saturated in serial 10%, 20%, and 30% sucrose in 1x PBS solutions at 4°C. Once saturated, brains were embedded in O.C.T. (Sakura Tissue-Tek® O.C.T. compound) for 30 min at room temperature, placed on dry ice to cure, then stored at -80°C until sectioning. Coronal brain sections of the hypothalamus were cut on a Leica CM3050S Cryostat at a thickness of 40 μm and mounted in parallel series on Fisherbrand Superfrost Plus ™ microscope slides and stored at -80 °C until further use.

Slides containing brain sections that included the supraoptic nucleus were identified using the optic chiasm as a landmark.[33,46] Selected slides were dried for 30 min in a 37°C incubator. The slides were washed three times with PBS for 10 min each. Three antigen retrieval steps were performed[47]: 10 min in 1% H_2O_2 and 1% NaOH in PBS, 10 min in 0.3% glycine in PBS, and 10 min in 0.03% SDS in PBS. Slides were blocked with 5% Normal Goat Serum (NGS; Abcam AB138478) in 0.5% PBS-Tween20 (PBST) for 1 h at room temperature. Slides were then incubated for 48 h at 4°C with rabbit anti-AVP (1:1000 dilution, Millipore AB1565, RRID: AB_90782) and mouse anti-c-Fos (1:500 dilution, Santa Cruz sc-271243) in 2% NGS in 0.1% PBST. Primary antibodies were refreshed after 24 h. After 48 h, the slides were washed with 0.1% PBST. Slides were then incubated with Goat anti-rabbit Alexa Fluor 555 (1:1000) and Goat anti-mouse Alexa Fluor 488 (1:400) in 0.1% PBST for 2 h at room temperature. The slides were washed with 0.1% PBST and rinsed with 1x PBS. Slides were mounted with Vectashield containing DAPI (Vector Laboratories H-1200) and imaged on a Zeiss LSM 900 Airyscan 2 with Axio Observer Microscope, Axiocam 705 Camera, and Zeiss Zen 3.5 Blue Edition software.

For each animal, 3 to 4 confocal images were analyzed in ImageJ (FIJI Version 1.0).[42] Briefly, maximum intensity projection confocal images were split into red and green channels, and an appropriate threshold was determined for each channel by comparing several images taken from different animals. The same red and green channel thresholds were applied to all images from all animals. Once thresholded, the Cell Counter plugin was used to count AVP^+ neurons, $cFOS^+$ neurons, and AVP^+ $cFOS^+$ neurons.

Stereotaxic surgery

Animals were anesthetized using isoflurane in 100% O_2 (induction, 4%; maintenance, 1%–3%). Ophthalmic ointment (Optixcare) was applied to the eyes, the fur above the skull was shaved, and Lidocaine 2% (diluted 1:200, 100 μL) was injected subcutaneously into the skin above the skull. Buprenorphine HCl in sterile saline (0.03 mg/kg) was injected subcutaneously between scapulae before surgery. The animal was placed into a stereotaxic apparatus (Kopf, Model 940 Small Animal Stereotaxic Instrument with Digital Display Console) and ear bars were inserted to secure the skull.

For the duration of surgery, sterile technique was used, and the animal's heart rate and blood oxygen levels were monitored with a pulse oximeter (MouseStat Jr. with rat sensor). Body temperature was monitored and maintained at 37°C with a TCAT-2LV Animal Temperature Controller and heating pad (Physitemp). The scalp was swabbed with povidone-iodine solution (Betadine) followed by 70% ethanol several times. An incision was made in the skin to reveal the surface of the skull, and a dental drill (Foredom) with a 1.2 mm burr was used to create a hole in the skull large enough to accommodate the optic fiber.

To express the calcium indicator GCaMP6s in SON neurons, we injected 1 μL of AAV9.CaMKII.GCaMP6s.WPRE.SV40 virus (Addgene, #107790) unilaterally into the SON at a speed of 0.1 μL/min using a Nanoject III™ Programmable Nanoliter Injector (Drummond Scientific) with pulled glass pipettes that had tip diameters of 10-20 μm. Injection coordinates for squirrel SON were 1.5 mm lateral, 8.6 mm deep, and between 7.16-8.86 mm anterior to ear bar (corresponding to 0.21-1.01 mm anterior to bregma).

In the same surgery, a fiber optic cannula (MFC_400/430-0.66_10mm_MF2.5_FLT, Doric) was lowered at a rate of 0.2 mm/min to 8.6 mm and secured to the skull using Relyx Unicem 2 Automix Syringe Resin Cement (3M). The skin above the skull was sutured using Michel Suture clips (Fine Science Tools). Immediate postoperative analgesia included meloxicam (0.2 mg/kg bw) in 1.5 mL of sterile saline delivered subcutaneously. Thereafter, buprenorphine HCl (0.01 mg/kg bw) and meloxicam (0.1 mg/kg bw) were given every 12 h for 48 h.

Please cite this article in press as: Junkins et al., Neural control of fluid homeostasis is engaged below 10°C in hibernation, Current Biology (2024), https://doi.org/10.1016/j.cub.2024.01.035

After 5 weeks post-surgery while squirrels were still in the active state, fiber photometry recordings were performed to assess viral expression. Those that had high GCaMP signal quality, high intensity (~100 mV), and dynamic changes in signal intensity were moved into the hibernaculum between mid-August and late September to induce hibernation. All animals entered hibernation between late August and early October.

Fiber photometry

Fiber photometry squirrels were allowed to hibernate uninterrupted for 4 weeks before the first recording, experiencing a minimum of 4 torpor bouts and a maximum of 8. Once this period had passed, recordings were made after several days in torpor since the previous IBA bout (minimum of 4 days in torpor, maximum of 22). All squirrels were tested 3 times during hibernation in the same order: first without treatment, then with 2 M NaCl, and finally with 3 M NaCl intraperitoneally (i.p.). After each test, squirrels were allowed to re-enter torpor, go through at least 1 natural bout of IBA, and re-enter torpor again for at least 4 days before the next recording. All recordings were made between September and January, corresponding to a minimum of 4 torpor bouts and maximum of 16.

For each recording, a torpid squirrel was brought to the room containing the fiber photometry setup, which is maintained at room temperature. The squirrel was removed from its hibernation box, weighed, and held while the fiber optic cannula was cleaned and then connected to the patch cord. After connecting the patch cord to the optic fiber, the squirrel was allowed to arouse over the course of 1-2 h. For osmosensory experiments, the squirrel was injected with 500 μL of either 2 M or 3 M NaCl i.p. immediately prior to the start of recording while the animal was still torpid. Throughout the session, T_B was measured every 5 minutes with a temperature transponder reader (BMDS) and recorded. After T_B reached >35°C, the experiment ended, and the animal was brought to the hibernaculum and allowed to re-enter hibernation before being tested again at the end of a later torpor bout. After 2 M experiments, we returned animals to the hibernaculum with ad libitum access to water for 24 h to allow them to re-establish fluid homeostasis before the next 3 M fiber photometry experiment. All animals re-entered torpor within 1-3 days.

The fiber optic cannula for Squirrel 223002 (Figure S1E) broke and was not able to be repaired before it could be tested for 2 M or 3 M NaCl. The No Treatment data for this squirrel was still included in Figures 4B and 4D. Thus, we obtained n = 7 for No Treatment and n = 6 for 2 M and 3 M NaCl in Figure 4D.

Using RZ10x Expanded Lux10 Processor and Tucker-Davis Technologies Synapse Version 96 software, two channels were recorded. Channel 1: LX405 Cable, FP200URT-TDT-2M-SP 200 μM 0.5 NA, 405 nm using parameters: Max 200 mA, Frequency 210 Hz, Level 30 mA, DC Offset 5 mA. Channel 2: LX465 Cable, FP200URT-TDT-2M-SP 200 μM 0.5 NA, 465 nm using parameters: Max 200 mA, Frequency 330 Hz, Level 30 mA, Offset 7 mA. Signal quality was >98% at the onset of recording.

At the end of the last experiment (3 M NaCl injection), animals were sacrificed by isoflurane overdose, perfused, and the brain was collected for immunohistochemistry and verification of optic fiber placement. Immunohistochemistry and confocal imaging protocols were identical to those described above (see "Immunohistochemistry"), with one exception: instead of staining for cFOS, native GCaMP fluorescence was sufficient to detect colocalization with AVP.

Data analysis for fiber photometry

Fiber photometry data analysis was performed in MATLAB (version R2023a). Briefly, the GCaMP (465 nm) and isosbestic (405 nm) data streams were imported from TDT using the TDTbin2mat function. Data were downsampled 1000x by averaging around every 1000th point. To normalize the GCaMP data, the isosbestic data was subtracted from the GCaMP signal, which was then z-score normalized using the normalize function. The z-score was derived by subtracting the mean of the data and then dividing by the standard deviation. This z-score normalization was performed on each squirrel for each treatment. This conversion of the data to a standardized scale with a mean of zero and a standard deviation of one allowed for more direct comparison of the GCaMP signals across individuals and all three different experimental conditions. To visualize the effects of 2 M and 3 M NaCl injections on *in-vivo* neuronal activity compared to no treatment control conditions, we plotted the means ± standard error of the mean for the first 400 s of each experiment. For statistical analysis, we performed linear mixed model using the lme4 package followed by Tukey pairwise comparison using the emmeans package in R.

QUANTIFICATION AND STATISTICAL ANALYSES

Statistical analyses were performed in GraphPad Prism 10.0 (GraphPad Software) and R (R version 4.0.2). Tests were chosen based on normality, data distribution and experimental design, and detailed accordingly in the results section and figure legends. Sample sizes for each experiment are noted and described in figure legends.

Current Biology, Volume *34*

Supplemental Information

Neural control of fluid homeostasis is engaged below 10°C in hibernation

Madeleine S. Junkins, Ni Y. Feng, Lyle A. Murphy, Genevieve Curtis, Dana K. Merriman, Sviatoslav N. Bagriantsev, and Elena O. Gracheva

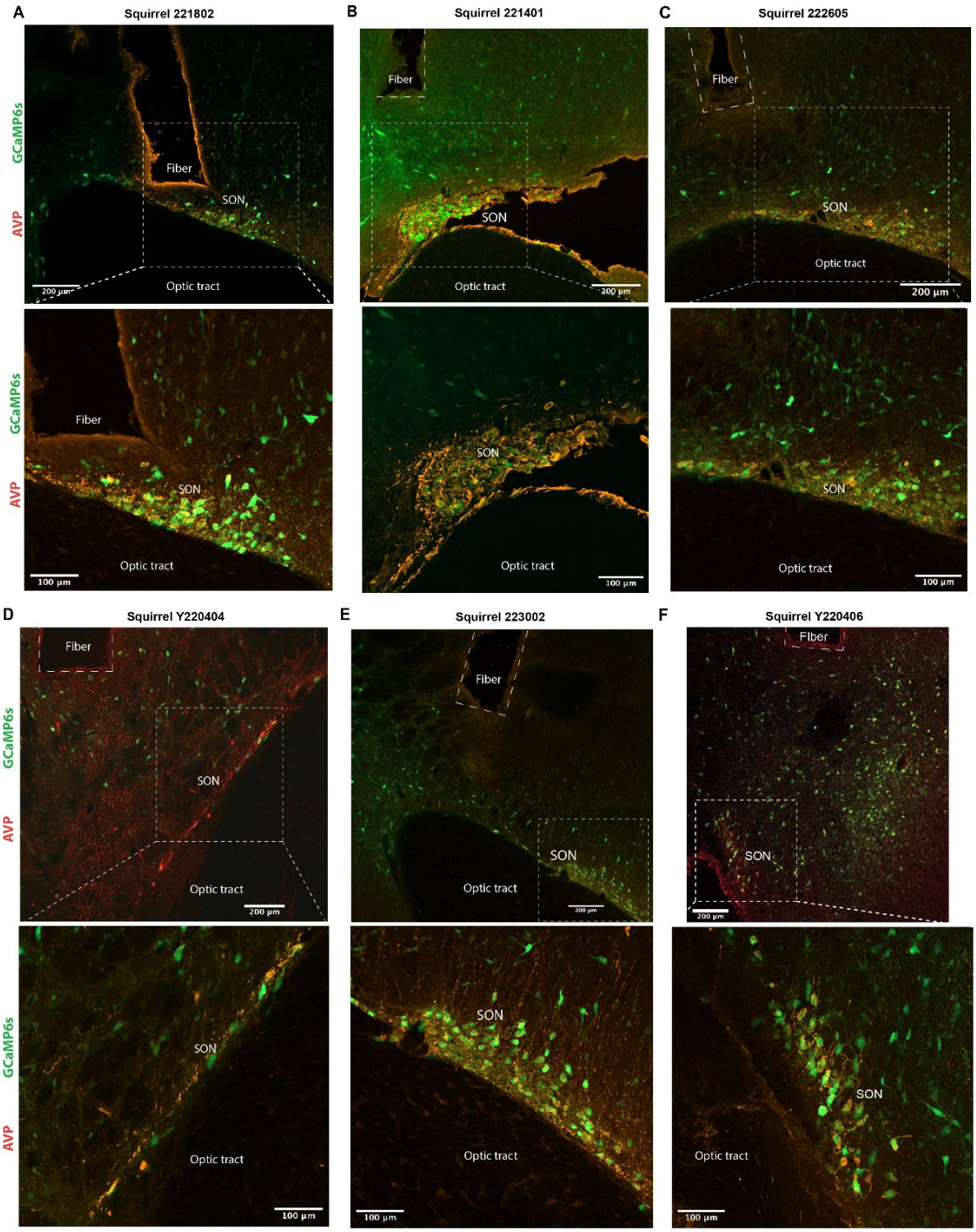

Figure S1. Verification of optic fiber placement and co-localization of AVP and GCaMP6s in SON. Related to Figure 4. Images showing AVP$^+$ cells (immunostaining; red), GCaMP6s$^+$ cells (native fluorescence; green), and the position of the optical fiber in SON of the 6 additional squirrels included in the datasets presented in Figure 4B, D. Insets show high-magnification images of the areas outlined by the dotted white line containing AVP$^+$ SON neurons.

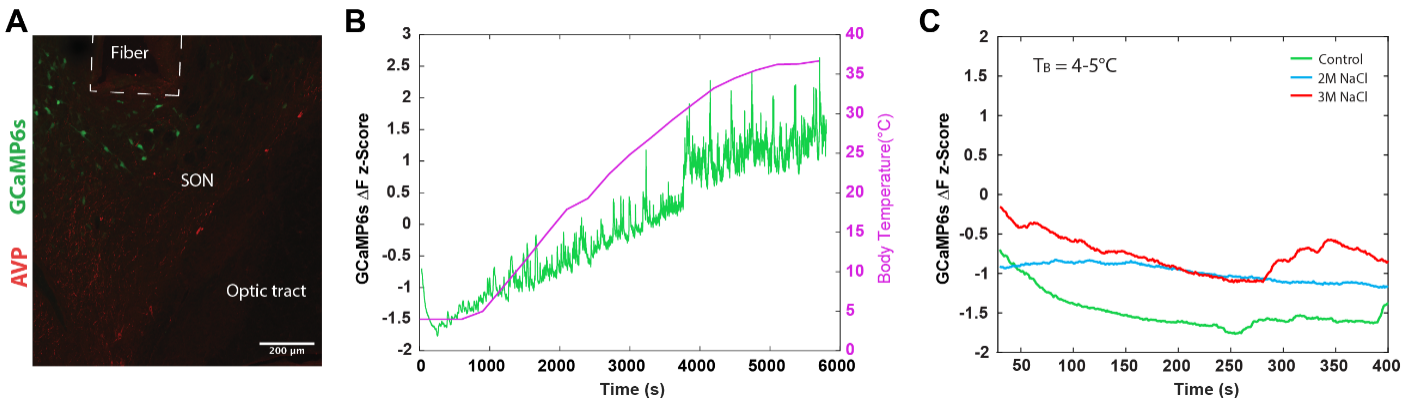

Figure S2. Optic fiber placement and fiber photometry from AVP^{-} neurons outside of SON. Related to Figure 4.

(A) SON image showing AVP-expressing cells (immunostaining; red) non-overlapping with GCaMP6s-epxressing cells (native fluorescence; green). The position of the optical fiber is indicated.

(B) Simultaneous recordings of GCaMP6s fluorescence in SON (green, left axis) at different T_B (pink, right axis) during arousal of an animal with non-overlapping AVP and GCaMP6s neurons.

(C) Intraperitoneal injection of hyperosmotic solutions fails to stimulate an increase in fluorescence at T_B = 4-5°C in SON from an animal with non-overlapping AVP and GCaMP6s neurons.

Figure / Experiment	**Active**	**Torpor**	**10°C**	**27°C**	**32°C**	**IBA**	**Entire Torpor-Arousal Transition**
Figure 1B Serum Osmolality	12F 23M	4F 11M	4F 8M	3F 4M		14F 12M	
Figure 1C Plasma OXT	4F 8M	8F 6M	1F 5M	2F 4M		3F 8M	
Figure 1D Plasma AVP	3F 6M	6F 6M	1F 5M	2F 4M		3F 6M	
Figure 2A-C Pituitary EM	2F 1M	2F 1M	1M 1F		2F 0M	0F 4M	
Figure 2D Pituitary OXT	0F 6M	4F 5M	1F 3M			3F 3M	
Figure 2E Pituitary AVP	3F 3M	2F 2M	3F 4M			3F 3M	
Figure 3A-C RNA-Seq	3F 2M	1F 4M				1F 4M	
Figure 3D SON IHC	2F 2M	1F 3M	2F 2M	2F 2M		4F 0M	
Figure 4B-D Fiber Photometry (cont.)							4F 3M
Figure 4D Fiber Photometry (2M/3M)							3F 3M

Table S1. The number of females (F) and males (M) in each group for each experiment. Related to STAR Methods.